Research Article

A new peltospirid snail (Gastropoda: Neomphalida) adds to the unique biodiversity of Longqi vent field, Southwest Indian Ridge

Chong Chen[1*], Yuru Han[2], Jonathan T. Copley[3], Yadong Zhou[2,4*]

[1] *X-STAR, Japan Agency for Marine-Earth Science and Technology (JAMSTEC), 2-15 Natsushima-cho, Yokosuka, Kanagawa, 237-0061, Japan*

[2] *Key Laboratory of Marine Ecosystem Dynamics, Second Institute of Oceanography, Ministry of Natural Resources, Hangzhou, China*

[3] *Ocean & Earth Science, University of Southampton, Waterfront Campus, European Way, Southampton SO14 3ZH, United Kingdom*

[4] *Southern Marine Science and Engineering Guangdong Laboratory (Zhuhai), Zhuhai 519082, China*

* Corresponding authors. E-mail: CC, cchen@jamstec.go.jp; YZ, yadong_zhou@sio.org.cn

Abstract

Biodiversity of deep-sea hydrothermal vents in the Indian Ocean remains poorly characterised compared with their Pacific and Atlantic counterparts. Although the Longqi hydrothermal vent field is the most extensively explored vent site on the ultraslow-spreading Southwest Indian Ridge, it is still a constant source of new discoveries. Here, we report and formally describe a new peltospirid snail from Longqi – *Lirapex felix* n. sp. Known from only two specimens, it differs from other named *Lirapex* species by a depressed spire and the lack of coil loosening on the adult body whorl. Examinations of the external anatomy and radular characteristics agree with its placement in *Lirapex*, also supported by a molecular phylogeny reconstructed using the barcoding fragment of the mitochondrial cytochrome *c* oxidase I (COI) gene. This is the fifth peltospirid snail known to inhabit the Longqi field, of which three including *Lirapex felix* n. sp. have been found nowhere else. There is growing evidence that the Longqi field represents a biogeographically unique site among Indian Ocean vents. The discovery of *Lirapex felix* n. sp. adds to the unique biodiversity of Longqi field, with implications for conservation in the light of potential deep-sea mining.

Keywords: Mollusca, deep-sea, hydrothermal vent, Indian Ocean, new species

This work is registered in ZooBank under: urn:lsid:zoobank.org:pub:3B892762-2110-4A1E-A80D-1779CBEC5EB3

Introduction

Deep-sea hydrothermal vents host lush communities of animals relying on microbial chemosynthetic primary production, using reducing compounds such as hydrogen sulfide and methane in the hot vent fluid as energy sources (Van Dover, 2000). Only around 600 of these underwater oases have been confirmed in the world since its discovery in 1977 (Corliss, 1979; Beaulieu & Szafrański, 2020), with most of the research and sampling done in Pacific and Atlantic Oceans (Thaler & Amon, 2019). Locating the first Indian Ocean vent had to wait until the 21st Century (Van Dover *et al*., 2001), and even now only about 10 active vents have been found (Sun *et al*., 2020; Wang *et al*., 2020a). Three of these are on the ultra-slow spreading Southwest Indian Ridge, including Longqi, Duanqiao, and Tiancheng hydrothermal vent fields (Copley *et al*., 2016; Zhou *et al*., 2018). Longqi and Tiancheng are relatively well-characterised compared with Duanqiao, which has not been visited by a submersible to date (Zhou *et al*., 2018).

The presence of local energy production makes hot vents very different from most deep-sea habitats in supporting a much higher biomass, but the 'extreme' environmental conditions in vents mean only taxa that have evolved appropriate adaptations are able to thrive. Due to this, over 70% of species found in vents are endemics that cannot live anywhere else (Wolff, 2005). At the same time, vents are also home to polymetallic sulfides, and are being targeted for deep-sea mining (Van Dover *et al.*, 2018). The majority of hydrothermal vents in the Indian Ocean, including all three on the Southwest Indian Ridge, are in the international waters and within areas licenced for mineral exploration by the International Seabed Authority. This has recently led many Indian Ocean vent species to become listed as Vulnerable, Endangered, or Critically Endangered on the IUCN (International Union for Conservation of Nature) Red List of Threatened Species (Sigwart *et al*., 2019).

Molluscs account for about a third of described hot vent biodiversity, of which approximately two-thirds are vent endemics (Wolff, 2005; Chapman *et al*., 2019). A number of molluscan families specialise in chemosynthetic ecosystems, including not only vents but also hydrocarbon seeps and organic falls, such as the three families in the gastropod order Neomphalida – Neomphalidae, Melanodrymiidae, and Peltospiridae (McLean, 1989; Heß *et al*., 2008). Of these, the family Peltospiridae is even more specialised, being endemic to hot vents (Chen *et al*., 2015a). Four peltospirid species, all in different genera, are known from the Indian Ocean (Chen *et al*., 2017a); among them

only the Scaly-foot Snail *Chrysomallon squamiferum* Chen *et al*., 2015b is widely distributed across multiple mid-oceanic ridges, while the other three are constrained to the Southwest Indian Ridge (Zhou *et al*., 2018; Sun *et al*., 2020). These include *Gigantopelta aegis* Chen *et al*., 2015a currently recorded from Longqi field and the nearby Duanqiao field, as well as *Dracogyra subfusca* Chen *et al*., 2017a and *Lirapex politus* Chen *et al*., 2017a which have not been found outside Longqi.

Chrysomallon and *Gigantopelta* are giant peltospirids (reaching 50 mm compared to typically less than 10 mm in other genera) relying on endosymbiotic bacteria (Goffredi *et al*., 2004; Heywood *et al*., 2017). The Longqi field (Fig. 1) is characterised by a peltospirid-dominated assemblage, with *G. aegis* being the dominating species and *C. squamiferum* being less abundant but closer to sources of vent fluids (Chen *et al*., 2015a; Copley *et al*., 2016; Zhou *et al*., 2018). The two smaller, grazing or deposit-feeding species *D. subfusca* and *L. politus* live among the two symbiotic species, and are also usually found in high densities (Chen *et al.,* 2017a). This peltospirid-dominated assemblage is unique to Longqi, which lacks a number of dominant megafaunas (e.g., the hairy snail *Alviniconcha marisindica* Okutani in Johnson *et al*., 2014, the vent crab *Austinograea rodriguezensis* Tsuchida & Hashimoto, 2002) found in other Indian Ocean vents further east, including Tiancheng on the same ridge (Sun *et al*., 2020).

When carrying out further sorting of material collected at Longqi during the Chinese expedition DY35 on-board R/V *Xiangyanghong 9* with the Human Occupied Vehicle (HOV) *Jiaolong* targeting other taxa, we unexpectedly encountered a single specimen of peltospirid snail morphologically distinct from the four described Indian Ocean species, from the same peltospirid-dominated assemblage. This prompted us to re-examine materials collected during the British RRS *James Cook* expedition KC67 using the Remotely Operated Vehicle (ROV) *Kiel6000*, an effort which fortunately resulted in one additional specimen. Here, we characterise this newly found peltospirid snail using an integrated taxonomy approach combining morphology and genetics.

Materials and Methods

Collection and Preservation

The newly discovered peltospirid snail was recovered from washings of an assemblage dominated by the giant peltospirid snail *Gigantopelta* aegis mixed with the Scaly-foot

Snail *Chrysomallon squamiferum* on 'Tiamat' chimney (HOV *Jiaolong* Marker DFF11), Longqi hydrothermal vent field, Southwest Indian Ridge (Fig. 1; also see Copley *et al*., 2016). One specimen was found in a sample preserved in 95% ethanol taken using a scoop by HOV *Jiaolong* during dive DV94 on-board R/V *Xiangyanghong 9* expedition DY35. A second specimen was found in a sample preserved in 99% ethanol taken using a suction sampler on ROV *Kiel6000* during the RRS *James Cook* expedition JC67.

Morphology

Specimens were observed and dissected under a stereo dissecting microscope (Carl Zeiss SteREO Discovery V.12), and photographs were taken using a digital single lens reflex camera (Nikon D5000) mounted on the trinocular. Shell measurements were taken using a digital calliper, numbers reported are rounded up to one decimal point. The head-foot of one specimen (collected in expedition DY35) was extracted using fine forceps and used for DNA sequencing after removing the radula sac for electron microscopy. Shell of the second specimen (collected during expedition JC67) was broken from the aperture after photography to generate a number of shell pieces with fresh fractured surfaces, for electron microscopy of the shell microsculpture. The rest of the shell was then dissolved using 1 mol/L hydrochloric acid solution in order to safely extract the soft parts for examination of external anatomy. Since the animal was dehydrated in 99% ethanol, the soft parts were subjected to rehydration in MilliQ water for 24 hours before observation and photography under the same dissecting microscope.

Electron Microscopy

The radula sac of the specimen collected in expedition DY35 was placed in diluted commercial bleach for a couple of minutes after dissection, in order to dissolve the tissue surrounding the radula. The shell apex of the same specimen was covered by a layer of sulfide mineral deposits. To reveal the protoconch, diluted commercial bleach was applied to the deposit layer for softening and then it was carefully peeled using fine tungsten needles. The operculum of the specimen collected in expedition JC67 was removed and cleaned using diluted commercial bleach, along with pieces of the shell broken for microstructure observations. Specimens were washed in MilliQ water twice and 99% ethanol twice after bleach treatments, and then mounted on scanning electron microscopy (SEM) stubs with carbon tapes. They were then air-dried and observed uncoated at 15 kV using a Hitachi TM-3000 SEM.

Genetics

Extraction of genomic DNA was performed on the DY35 specimen using the DNeasy blood and tissue kit (Qiagen, CA, USA), following standard protocols supplied by the manufacturer. Partial sequence of mitochondrial cytochrome oxidase *c* subunit I (COI) gene in the standard metazoan barcoding region was amplified using the universal primer pair HCO2198/LCO1490 (Folmer *et al*., 1994) following the amplification procedures described in Zhou *et al*. (2018). Amplicons were purified using the Cycler kit (OMEGABio-tec) following the manufacturer's protocols and then submitted to bi-directional Sanger sequencing in the company BioSune (Shanghai, China). The consensus sequence was assembled in the software Geneious R11 (https://www.geneious.com) and then used in downstream analyses. This newly generated sequence is deposited on NCBI GenBank under the accession number MW452523.

Phylogenetic reconstruction was undertaken using COI sequences of Neomphalida species available on GenBank following Chen *et al*. (2017a), and using the distantly related vetigastropod *Turbo sazae* Fukuda, 2017 as the outgroup. The sequences were aligned in Geneious R.11 and the alignment length used for phylogenetic inferences was 570 bp. PartitionFinder v2.1.1 (Lanfear *et al*., 2017) was used to select the substitution model with the Bayesian information criterion, which selected the GTR+I+G model for all codons. Phylogeny was reconstructed using Bayesian inference in MrBayes v3.2.6 (Ronquist *et al*., 2012) with Metropolis-coupled Monte Carlo Markov chains run for one million generations and topologies sampled every 100 generations. Tracer v1.6 (Rambaut *et al*., 2013) was used to decide an adequate burn-in value, this being 2500 in our case. The software package MEGA7 (Kumar *et al*., 2016) was used to estimate pairwise distances of COI sequences, using the K2P distance (Kimura, 1980).

Type Repositories

Type specimens are deposited at the Repository of the Second Institute of Oceanography (RSIO), Ministry of Natural Resources, Hangzhou, China and the National Museum of Nature and Science, Tsukuba (NSMT), Japan.

Results

Systematics

Order Neomphalida McLean, 1990

Superfamily Neomphaloidea McLean, 1981

Family Peltospiridae McLean, 1989

Lirapex Warén & Bouchet, 1989

Type species: *Lirapex humatus* Warén & Bouchet, 1989 (by original designation).

Diagnosis: Small to medium sized (< 5 mm) coiled peltospirid snails with skeneiform shells. Shell sculpture ranging from smooth to carrying distinct axial sculpture that is strongest at shoulder and umbilicus. Protoconch with distinct spiral ridges on the posterior part which disappear towards the anterior half. Radula with hook-like marginals. Film-like multispiral operculum present. Sexes separate. Tentacles smooth, not modified into copulatory organ. Snout of even breadth. Epipodial tentacle only present around opercular attachment (Warén & Bouchet, 1989; Warén & Bouchet, 2001; Chen *et al*., 2017a).

Lirapex felix n. sp.

Figs. 2-4

ZooBank registration: urn:lsid:zoobank.org:act:7BE47DEC-FB80-473F-8658-2C268ED67627

Diagnosis: Lirapex with depressed spire (shell height to width ratio 1:1.2 in both specimens known) and tightly coiled, non-disjunct final whorl. Sculpture consisting of weak axial ribs up to 100 μm apart on the teleoconch, strength somewhat variable but strongest at shoulder and base.

Type locality: 'Tiamat' chimney (HOV *Jiaolong* Marker DFF11), Longqi vent field, Southwest Indian Ridge.

Type material: Holotype (RSIO 35733; Fig. 2A-D, 2I, 3A-B), male, shell width 2.6 mm, shell height 2.1 mm, in 95% ethanol, Longqi vent field, Southwest Indian Ridge, 37° 47.03' S / 49° 39.01' E ('Tiamat' Chimney / DFF11), 2761 m deep, R/V *Xiangyanghong* 9 expedition DY35, HOV *Jiaolong* Dive 94, 2015/i/11. Used for DNA sequencing and the examination of radula and teleoconch sculpture under SEM.
Paratype (NSMT-Mo XXXXXX; Fig. 2E-H, 3C-F), female, shell width 3.7 mm, shell height 3.1 mm, 99% ethanol, Longqi vent field, Southwest Indian Ridge, 37°47.03' S /

49°38.97'E ('Tiamat' Chimney / DFF11), 2785 m deep, RRS *James Cook* expedition JC67, ROV *Kiel6000* Dive 142, 2011/xi/29. Shell dissolved for the examination of external anatomy after pieces broken for SEM observation of microstructure.

Description: Shell (Fig. 2) fairly solid, depressed skeneiform, much wider than tall, shell height to ratio approximately 1:1.2. Known maximum dimensions width 3.7 mm, height 3.1 mm (Paratype specimen). Tightly coiled, no evidence of coil loosening even in final whorl. Typically encrusted by mineral deposits. Protoconch (Fig. 3A) approximately 0.5 whorl, diameter 240 μm. Five distinct spiral ridges with finer spiral wrinkles present on posterior half, anterior half completely smooth. Transition to teleoconch marked by clearly thickened ridge. Teleoconch with three whorls, white in colouration, covered by semi-transparent, greenish periostracum. Teleoconch sculpture (Fig. 3B) consisting of more-or-less equidistant, weak, axial ribs up to 100 μm apart. Rib strength vary somewhat, but always evident on shoulder or base near umbilicus where it is strongest. Whorls nearly round in cross section, aperture not thickened in adults. Umbilicus opening of moderate size. Shell microstructure (Fig. 3F) non-nacreous, comprising two layers. Granular layer on outside much thinner than cross-lamellar layer on inside, latter being partly penetrated by shell pores, which taper towards granular layer but diminishes before transition.

Operculum (Fig. 3C) multispiral, approximately 12 volutions in adult specimen (paratype), thin film-like, semi-transparent. Later volutions form clear extending fringes overlapping over subsequent volution.

Radula (Fig. 3D-E) rhipidoglossate, with formula ~25 + 4 + 1 + 4 + ~25. Rachidian and laterals well-reinforced. Rachidian tooth triangular, sides slightly sigmoidal in outline, with triangular overhanging cusp, cutting edge smooth. Base of rachidian trifurcated. Laterals with bifurcating reinforcement at base, all have triangular, overhanging cusps with up to five minor serrations on both sides. All laterals with single minor protuberance near base. Laterals become less laterally bent with progressively broader cusps from innermost to outermost, outermost lateral being much broader than others. Marginal teeth long, thin, distally tapered. Innermost marginals larger in size, gradually decreasing outwards. Marginal cusps hook-like, serrated into approximately 15 denticles.

Soft parts (Fig. 4) just shy of three volutions. Sexes separate. Head large, eyes lacking. Snout even in breadth, short, mouth ventral. Cephalic tentacles about 1.5 times as long as snout when observed in contracted state, conical, rapidly decreasing in size distally. Both

cephalic tentacles simple, smooth, no evidence of modification into copulation appendages in either sex. Cephalic lappets lacking, as well as neck-lobe. Foot well developed, transverse furrow separates propodium from mesopodium. Epipodial tentacles arranged in semi-circular fashion surrounding posterior two-thirds of opercular attachment, numbering 17 on either side, 34 in total. Pallial edge simple, lacking appendages. Columellar muscle reaching only approximately 0.3 whorls behind pallial edge, attachment area larger on right side than left side, two sides connected by a thick band of ventral muscular tissue.

Mantle cavity extending 0.4 whorls posterior of pallial edge. Ctenidium moderately large, bipectinate, approximately 35 leaflets. Digestive tract mostly filled with dark mineral deposits, especially intestine which loops twice between stomach and left kidney. Stomach clearly enlarged compared to intestine, located 0.9 whorls posterior from pallial edge. Rectum curves slightly after entering mantle cavity, attached on mantle ceiling, becoming detached just posterior of anus. Heart monotocardian, ventricle located posteroventrally compared to auricle. Pericardium not penetrated by intestine (seen by transparency). Visceral mass dorsally occupied by digestive gland extending up to apex, ventrally occupied by gonad. Gonopore simple, located behind anus.

Distribution: So far only known from the Longqi hydrothermal vent field, Southwest Indian Ridge, Indian Ocean. It lives in association with giant peltospirid species *Chrysomallon squamiferum* and *Gigantopelta aegis* on the active diffuse-flow chimney 'Tiamat'.

Etymology: '*Felix*' (adjective, Latin), meaning lucky, happy, or blessed. It is named in reference to the serendipitous discovery of the first specimen of this apparently rare species and the fortunate discovery of the second specimen that allowed for a comprehensive description.

Remarks: The placement of *L. felix* n. sp. in *Lirapex* is supported by 1) a coiled shell; 2) radula with outer marginals possessing serrated, hook-like cusps, and outermost lateral tooth much broader than the rest; 3) protoconch with distinct spiral ridges; 4) anterior part of the intestine visible in two coils between the stomach and the left kidney; 5) epipodial tentacles only present around the opercular attachment.

Four other species are currently recognised in the genus *Lirapex*. These include *L.*

humatus Warén & Bouchet, 1989 and *L. granularis* Warén & Bouchet, 1989 from East Pacific Rise, *L. costellatus* Warén & Bouchet, 2001 from Mid-Atlantic Ridge, and *L. politus* Chen *et al*., 2017a also from the Longqi field, Southwest Indian Ridge. *Lirapex felix* n. sp. can be distinguished from all four by its more depressed shell form and the fact that there is no evidence of the coil loosening in the final whorl, an unusual feature among *Lirapex* species. In *L. humatus* and *L. costellatus* the second half of the adult body whorl is clearly detached from the previous whorl (Warén & Bouchet, 1989; Warén & Bouchet, 2001), whereas in *L. granularis* and *L. politus* the whorl does not detach but visibly loosens (Warén & Bouchet, 1989; Chen *et al*., 2017a). Apart from *L. felix* n. sp. which is wider than tall, all described *Lirapex* species are typically as tall as wide or taller than wide (Warén & Bouchet, 2001; Chen *et al*., 2017a). Although these are the results from only observing two specimens of *L. felix* n. sp., at least the paratype specimen is fully mature and the characters are likely reliable.

The shell sculpture of *L. felix* n. sp. is similar to that observed in *L. humatus* and *L. costellatus*. In both *L. humatus* and *L. costellatus* the sculpture is highly variable in development and may be present all over the shell surface or only between the shoulder and base (Warén & Bouchet, 1989; Warén & Bouchet, 2001). Even in the two specimens of *L. felix* n. sp. available the sculpture differed in strength, being stronger in the holotype than the paratype specimen, suggesting that the sculpture strength could be as variable as those two species. Unlike these three species, the granular sculpture of *L. granularis* is only present on the periostracum and the teleoconch is smooth (Warén & Bouchet, 1989), making it impossible to confuse with *L. felix* n. sp. Similarly, both teleoconch and periostracum of *L. politus* are completely smooth (Chen *et al*., 2017a), and thus it cannot be confused with the co-occurring *L. felix* n. sp. The radula of *L. felix* n. sp. has a smooth rachidian cusp similar to *L. costellatus* and *L. politus*, but differ from *L. humatus* which has a serrated rachidian cusp (Warén & Bouchet, 2001; Chen *et al*., 2017a).

Genetic Support

The reconstructed consensus tree generated by Bayesian inference using the barcoding fragment of the COI gene is presented in Figure 5. The order Neomphalida (and therefore superfamily Neomphaloidea) was recovered as a fully supported clade (Posterior Probability, PP = 1). In the present phylogeny, Melanodrymiidae (represented by *Melanodrymia*, *Leptogyra,* and *Leptogyropsis*) was recovered as a monophyletic clade, whereas Neomphalidae (represented by *Cyathermia* and *Lamellomphalus*) and Peltospiridae (represented by *Chrysomallon, Depressigyra, Gigantopelta, Peltospira,*

Nodopelta, Rhynchopelta, Dracogyra, Pachydermia, and *Lirapex*) were not recovered as monophyletic. Nevertheless, the placement of *Lirapex felix* n. sp. in Neomphalida can be confirmed. The topology does not contradict its placement in *Lirapex*, being recovered sister to *L. politus* among the species included, making up a monophyletic genus *Lirapex* (although not strongly supported with PP < 0.7). *Lirapex* was recovered sister to *Pachydermia*, another genus currently placed in Peltospiridae (albeit also with low support), supporting its placement in Peltospiridae. Although recovered sister to *L. politus*, the K2P genetic distance between *L. felix* n. sp. and *L. politus* is rather large at 17.4% over 570 bp.

Discussion

Peltospiridae in Indian Ocean

The discovery of *Lirapex felix* n. sp. increases the peltospirid diversity in Longqi hydrothermal field and the Indian Ocean to five species, of which three (*L. felix* n. sp., *L.* politus, and *Dracogyra subfusca*) are restricted to Longqi and one is additionally found in the nearby Duanqiao field less than 80 km away (*Gigantopelta aegis*; Zhou *et al*., 2018). Only in Longqi do the five peltospirids co-occur and within the same assemblage type, the large aggregations of the giant peltospirids *Chrysomallon squamiferum* and *Gigantopelta aegis* (Fig. 1B). Although we did not attempt to examine the stomach contents of *L. felix* n. sp. due to rarity of material, the lack of an enlarged oesophageal gland (seen by transparency) combined with sizeable intestine and stomach suggests deposit feeding or grazing like most peltospirids including other *Lirapex* species (Fretter, 1989; Warén & Bouchet, 1989; Warén & Bouchet, 2001; Chen *et al*., 2017a). This is also in agreement with the intestine being packed with dark material in *L. felix* n. sp., seen through transparency.

Only two specimens of *Lirapex felix* n. sp. being found from relatively concentrated collecting efforts at the 'Tiamat' chimney (DFF11) in the Longqi hydrothermal vent field (Copley *et al*., 2016; Zhou *et al*., 2018) suggests that it may be a rare species. Nevertheless, the relative abundance of *Lirapex politus* and *Dracogyra subfusca* have varied greatly between research cruises (Chen *et al*., 2017a), indicative of either waxing and waning of abundance between years or sampling bias associated with fine-scale habitat preferences. It is also possible that *L. felix* n. sp. is not truly rare but instead prefers a different microhabitat than *L. politus* where sampling has not been done, perhaps preferring more

sedimented areas like *L. humatus* (Warén & Bouchet, 1989). Future sampling efforts at Longqi and other Indian Ocean vents should pay careful attention to such microhabitats, in order to fully sample the biodiversity present.

Phylogeny

The overall topology of the molecular phylogeny presented herein (Fig. 5) is generally congruent with the tree presented in Chen *et al.* (2017), except that Melanodrymiidae was recovered as a monophyletic clade, although only weakly supported. Similar to recent previous analyses using the COI barcoding fragment (Chen *et al*., 2017; Zhang & Zhang, 2017), Neomphalidae and Peltospiridae continue to be recovered paraphyletic. Nevertheless, it has been known for a long time that the COI barcoding fragment is unable to fully resolve familial relationships within Neomphalida due to saturation (Heß *et al*., 2008; Chen *et al*., 2017b). Many nodes were also not well-supported in the COI phylogeny, echoing conclusions from previous studies that resolving the phylogeny within Neomphalida requires at least multi-gene approaches (Heß *et al*., 2008; Chen *et al*., 2017b). Neomphalidae and Peltospiridae are supported as monophyletic in a five-gene phylogeny (Chen *et al*., 2017b), and we therefore refrain from discussing familial assignment of neomphaloidean genera based on the tree presented herein. The genetic distance between the two *Lirapex* species included (*L. felix* n. sp. and *L. politus*) is rather large (K2P distance, 17.4% over 570 bp) for congeners, a phenomenon also known from some other neomphaloidean genera (Chen *et al.*, 2015b). For example, in the genus *Peltospira*, K2P distances among the three species included in the phylogeny herein range between 13.1-16.7% in K2P distance over the same 570 bp of the COI gene.

Implications for Conservation

There is growing evidence from population genetics that a dispersal barrier exists between Longqi and Tiancheng fields on the Southwest Indian Ridge, leading to a distinctive biological and genetic composition at Longqi (Copley *et al*., 2016; Zhou *et al*., 2018; Sun *et al*., 2020). The presence of *Gigantopelta* at East Scotia Ridge, along with other shared taxa between the two locations such as *Kiwa* yeti crabs, show that Longqi has been historically connected with East Scotia Ridge in a way that other Indian Ocean vents have not (Chen *et al*., 2015a; Roterman *et al*., 2016). The finding of *Lirapex felix* n. sp. in Longqi adds to this unique biodiversity. All other four peltospirid species in the Indian Ocean have been listed as Endangered or Critically Endangered on the IUCN Red List in the light of likely upcoming mining activities (Sigwart *et al*., 2019). Longqi field is located within a licence area for mineral exploration, and *Lirapex felix* n. sp. represents

yet another species with the need of conservation assessments and measures. Unlike some other species which were at least recorded in species lists prior to formal description (e.g., Wang *et al.*, 2020b), the presence of *L. felix* n. sp. was completely undetected prior to the present study, underlining the need for further sampling efforts to fully characterise the biodiversity in Longqi and other Indian Ocean vents.

Author Contributions

C.C. and Y.Z. conceived and designed the project. C.C., J.T.C., and Y.Z. collected and preserved the specimens used during their participation in the relevant research cruises. C.C. carried out morphological examinations of the specimens. Y.H. and Y.Z. carried out DNA sequencing, C.C., Y.H., and Y.Z. analysed the molecular data produced. C.C. interpreted the data and drafted the manuscript, after which all authors contributed to the final version.

Data Availability

Newly generated molecular data are deposited in NCBI GenBank under the accession number MW452523. Specimens used are deposited at the Repository of the Second Institute of Oceanography (RSIO), Ministry of Natural Resources, Hangzhou, China and the National Museum of Nature and Science, Tsukuba (NSMT), Japan.

Disclosure Statement

No potential competing interest was reported by the authors.

Funding

RRS *James Cook* cruise JC67 was supported by a United Kingdom Natural Environmental Research Council (NERC) Small Research Grant to J.T.C. (NE/H012087/1), and the R/V *Xiangyanghong 9* cruise by the Foundation of China Ocean Mineral Resources R & D Association (No. DYHC-125-35). C.C. was supported by a Grant-in-Aid for Scientific Research (KAKENHI) from the Japan Society for the Promotion of Science (JSPS) under the grant code 18K06401. This work was also supported an additional grant from the Foundation of China Ocean Mineral Resources R & D Association (No. DY135-E2-1-02) and a Scientific Research Fund of the Second Institute of Oceanography, Ministry of Natural Resources, China (Grant No. QNYC1902).

Acknowledgements

We thank the Master and crew of RRS *James Cook* and R/V *Xiangyanghong 9* for their tireless support of scientific activity on-board expeditions JC67 and DY35, respectively. We extend the same thanks to the pilots and technical teams of ROV *Kiel6000* and HOV *Jiaolong*, staff of the United Kingdom National Marine Facilities at the National Oceanography Centre for logistics and shipboard support, and all scientists on-board the expeditions. Yukiko Nagai (JAMSTEC) is thanked for her assistance in microscopy.

Figure Legends

Figure 1. A) Map of southwestern Indian Ocean showing the Longqi hydrothermal vent field on the Southwest Indian Ridge; **B)** 'Tiamat' chimney (DFF11) showing the typical peltospirid snail dominated aggregations alongside colonies of *Bathymodiolus* mussels and *Neolepas* stalked barnacles.

Figure 2. *Lirapex felix* n. sp., type specimens. **A-D)** Holotype (RSIO 35733); **E-H)** Paratype (NSMT-Mo XXXXXX); **I)** Close-up of the holotype near the umbilicus, showing the axial ribbing sculpture. Scale bars: **A-H** = 1 mm; **I** = 200 μm.

Figure 3. *Lirapex felix* n. sp., scanning electron micrographs. **A)** Protoconch, holotype (RSIO 35733), arrows indicating transition between protoconch and teleoconch; **B)** Shell sculpture, holotype (RSIO 35733); **C)** Operculum, paratype (NSMT-Mo XXXXXX); **D-E)** Radula, holotype (RSIO 35733); **F)** Shell microsculpture, arrows indicating shell pores. Scale bars: **A** = 100 μm; **B =** 200 μm; **C** = 1 mm; **D** = 50 μm; **E-F** = 20 μm.

Figure 4. *Lirapex felix* n. sp., soft parts, paratype (NSMT-Mo XXXXXX). **A)** Right view; **B)** Anterior view with part of the mantle roof removed, visceral mass digitally removed at the dashed line; **C)** Ventral view; **D)** Left view. Scale bars: **A, C-D** = 1 mm; **B** = 0.5 mm. Abbreviations: a, anus; c, ctenidium; d, digestive gland; et, epipodial tentacle; f, foot; i, intestine; k, left kidney; lm, left columellar muscle; ov, ovary; op, opercular attachment; p, pericardium; pe, pallial edge; r, rectum; rm, right columellar muscle; s, stomach; sn, snout; t, cephalic tentacle.

Figure 5. Consensus tree from phylogenetic reconstruction using Bayesian inference, based on 570 bp of the barcoding fragment of the mitochondrial COI gene. Node values

showing Bayesian Posterior Probabilities, only those above 0.7 are shown. GenBank accession numbers of the sequences used are indicated in parentheses.

References

Beaulieu SE, Szafra, ski KM (2020) InterRidge Global Database of Active Submarine Hydrothermal Vent Fields Version 3.4. PANGAEA. doi:10.1594/PANGAEA.917894

Chapman ASA, Beaulieu SE, Colaço A, Gebruk AV, Hilario A, Kihara TC, Ramirez-Llodra E, Sarrazin J, Tunnicliffe V, Amon DJ, Baker MC, Boschen-Rose RE, Chen C, Cooper IJ, Copley JT, Corbari L, Cordes EE, Cuvelier D, Duperron S, Du Preez C, Gollner S, Horton T, Hourdez S, Krylova EM, Linse K, LokaBharathi PA, Marsh L, Matabos M, Mills SW, Mullineaux LS, Rapp HT, Reid WDK, Rybakova E, A. Thomas TR, Southgate SJ, Stöhr S, Turner PJ, Watanabe HK, Yasuhara M, Bates AE (2019) sFDvent: A global trait database for deep-sea hydrothermal-vent fauna. Global Ecology and Biogeography 28:1538-1551 doi:10.1111/geb.12975

Chen C, Linse K, Roterman CN, Copley JT, Rogers AD (2015a) A new genus of large hydrothermal vent-endemic gastropod (Neomphalina: Peltospiridae). Zoological Journal of the Linnean Society 175:319-335 doi:10.1111/zoj.12279

Chen C, Linse K, Copley JT, Rogers AD (2015b) The 'scaly-foot gastropod': a new genus and species of hydrothermal vent-endemic gastropod (Neomphalina: Peltospiridae) from the Indian Ocean. Journal of Molluscan Studies 81:322-334 doi:10.1093/mollus/eyv013

Chen C, Zhou Y, Wang C, Copley JT (2017a) Two new hot-vent peltospirid snails (Gastropoda: Neomphalina) from Longqi hydrothermal field, Southwest Indian Ridge. Frontiers in Marine Science 4 doi:10.3389/fmars.2017.00392

Chen C, Uematsu K, Linse K, Sigwart JD (2017b) By more ways than one: Rapid convergence at hydrothermal vents shown by 3D anatomical reconstruction of *Gigantopelta* (Mollusca: Neomphalina). BMC Evolutionary Biology 17:62 doi:10.1186/s12862-017-0917-z

Copley JT, Marsh L, Glover AG, Hühnerbach V, Nye VE, Reid WDK, Sweeting CJ, Wigham BD, Wiklund H (2016) Ecology and biogeography of megafauna and macrofauna at the first known deep-sea hydrothermal vents on the ultraslow-spreading Southwest Indian Ridge. Scientific Reports 6:39158 doi:10.1038/srep39158

Corliss JB, Dymond J, Gordon LI, Edmond JM, von Herzen RP, Ballard RD, Green K, Williams D, Bainbridge A, Crane K, van Andel TH (1979) Submarine thermal springs on the Galápagos Rift. Science 203:1073-1083 doi:10.1126/science.203.4385.1073

Fretter V (1989) The anatomy of some new archaeogastropod limpets (Superfamily Peltospiracea) from hydrothermal vents. Journal of Zoology 218:123-169 doi:10.1111/j.1469-7998.1989.tb02530.x

Goffredi SK, Warén A, Orphan VJ, Van Dover CL, Vrijenhoek RC (2004) Novel forms of structural integration between microbes and a hydrothermal vent gastropod from the Indian Ocean. Applied and Environmental Microbiology 70:3082-3090 doi:10.1128/aem.70.5.3082-3090.2004

Heß M, Beck F, Gensler H, Kano Y, Kiel S, Haszprunar G (2008) Microanatomy, shell structure and molecular phylogeny of *Leptogyra*, *Xyleptogyra* and *Leptogyropsis* (Gastropoda: Neomphalida: Melanodrymiidae) from sunken wood. Journal of Molluscan Studies 74:383-401 doi:10.1093/mollus/eyn030

Heywood JL, Chen C, Pearce DA, Linse K (2017) Bacterial communities associated with the Southern Ocean vent gastropod, Gigantopelta chessoia: indication of horizontal symbiont transfer. Polar Biology 40:2335-2342 doi:10.1007/s00300-017-2148-6

Kimura M (1980) A simple method for estimating evolutionary rates of base substitutions through comparative studies of nucleotide sequences. Journal of Molecular Evolution 16:111-120 doi:10.1007/BF01731581

Kumar S, Stecher G, Tamura K (2016) MEGA7: Molecular Evolutionary Genetics Analysis Version 7.0 for Bigger Datasets. Molecular Biology and Evolution 33:1870-1874 doi:10.1093/molbev/msw054

Lanfear R, Frandsen PB, Wright AM, Senfeld T, Calcott B (2017) PartitionFinder 2: New Methods for Selecting Partitioned Models of Evolution for Molecular and Morphological Phylogenetic Analyses. Molecular Biology and Evolution 34:772-773 doi:10.1093/molbev/msw260

McLean JH (1989) New archaeogastropod limpets from hydrothermal vents: new family Peltospiridae, new superfamily Peltospiracea. Zoologica Scripta 18:49-66

Rambaut A, Suchard M, Drummond A (2013) Tracer v1.6. Available from http://treebioedacuk/software/tracer/

Ronquist F, Teslenko M, van der Mark P, Ayres DL, Darling A, Höhna S, Larget B, Liu L, Suchard MA, Huelsenbeck JP (2012) MrBayes 3.2: Efficient Bayesian Phylogenetic Inference and Model Choice Across a Large Model Space. Systematic Biology 61:539-542 doi:10.1093/sysbio/sys029

Roterman CN, Copley JT, Linse KT, Tyler PA, Rogers AD (2013) The biogeography of the yeti crabs (Kiwaidae) with notes on the phylogeny of the Chirostyloidea (Decapoda: Anomura). Proceedings of the Royal Society B: Biological Sciences 280:20130718 doi:10.1098/rspb.2013.0718

Sigwart JD, Chen C, Thomas EA, Allcock AL, Böhm M, Seddon M (2019) Red Listing can protect deep-sea biodiversity. Nature Ecology & Evolution 3:1134-1134 doi:10.1038/s41559-019-0930-2

Sun J, Zhou Y, Chen C, Kwan YH, Sun Y, Wang X, Yang L, Zhang R, Wei T, Yang Y, Qu L, Sun C, Qian P-Y (2020) Nearest vent, dearest friend: biodiversity of Tiancheng vent field reveals cross-ridge similarities in the Indian Ocean. Royal Society Open Science 7:200110 doi:10.1098/rsos.200110

Thaler AD, Amon D (2019) 262 Voyages Beneath the Sea: a global assessment of macro- and megafaunal biodiversity and research effort at deep-sea hydrothermal vents. PeerJ 7:e7397 doi:10.7717/peerj.7397

Van Dover CL (2000) The Ecology of Deep-Sea Hydrothermal Vents. Princeton University Press, Princeton

Van Dover CL, Arnaud-Haond S, Gianni M, Helmreich S, Huber JA, Jaeckel AL, Metaxas A, Pendleton LH, Petersen S, Ramirez-Llodra E, Steinberg PE, Tunnicliffe V, Yamamoto H (2018) Scientific rationale and international obligations for protection of active hydrothermal vent ecosystems from deep-sea mining. Marine Policy 90:20-28 doi:10.1016/j.marpol.2018.01.020

Van Dover CL, Humphris SE, Fornari D, Cavanaugh CM, Collier R, Goffredi SK, Hashimoto J, Lilley MD, Reysenbach AL, Shank TM, Von Damm KL, Banta A, Gallant RM, Götz D, Green D, Hall J, Harmer TL, Hurtado LA, Johnson P, McKiness ZP, Meredith C, Olson E, Pan IL, Turnipseed M, Won Y, Young CR, Vrijenhoek RC (2001) Biogeography and ecological setting of Indian Ocean hydrothermal vents. Science 294:818-823

Wang Y, Han X, Zhou Y, Qiu Z, Yu X, Petersen S, Li H, Yang M, Chen Y, Liu J, Wu X, Luo H (2020a) The Daxi Vent Field: An active mafic-hosted hydrothermal system at a non-transform offset on the slow-spreading Carlsberg Ridge, 6°48′N. Ore Geology Reviews:103888 doi:10.1016/j.oregeorev.2020.103888

Wang Z, Xu T, Zhang Y, Zhou Y, Liu Z, Chen C, Watanabe HK, Qiu J-W (2020b) Molecular phylogenetic and morphological analyses of the 'monospecific' Hesiolyra (Annelida: Hesionidae) reveal two new species. Deep Sea Research Part I: Oceanographic Research Papers 166:103401 doi:10.1016/j.dsr.2020.103401

Warén A, Bouchet P (1989) New gastropods from East Pacific hydrothermal vents. Zoologica Scripta 18:67-102 doi:10.1111/j.1463-6409.1989.tb00124.x

Warén A, Bouchet P (2001) Gastropoda and Monoplacophora from hydrothermal vents and seeps; new taxa and records. Veliger 44:116-231 doi:10.1111/j.1463-6409.1993.tb00342.x

Wolff T (2005) Composition and endemism of the deep-sea hydrothermal vent fauna. Cahiers de Biologie Marine 46:97-104

Zhang S, Zhang S (2017) A new genus and species of Neomphalidae from a hydrothermal vent of the Manus Back-Arc Basin, western Pacific (Gastropoda: Neomphalina). The Nautilus 131:76-86

Zhou Y, Zhang D, Zhang R, Liu Z, Tao C, Lu B, Sun D, Xu P, Lin R, Wang J, Wang C (2018) Characterization of vent fauna at three hydrothermal vent fields on the Southwest Indian Ridge: Implications for biogeography and interannual dynamics on ultraslow-spreading ridges. Deep Sea Research Part I: Oceanographic Research Papers 137:1-12 doi:10.1016/j.dsr.2018.05.001

Figure 1

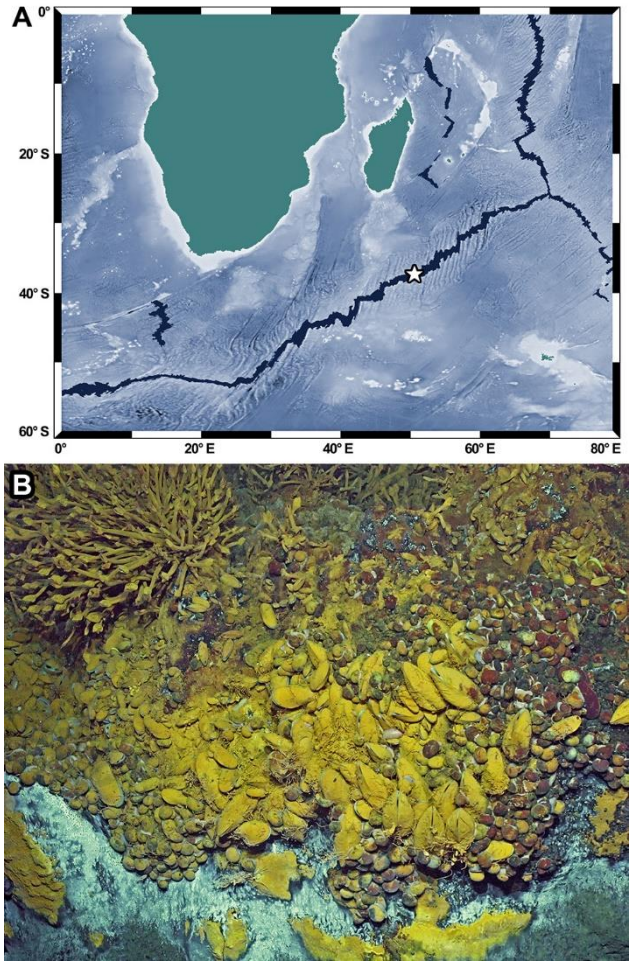

Figure 2

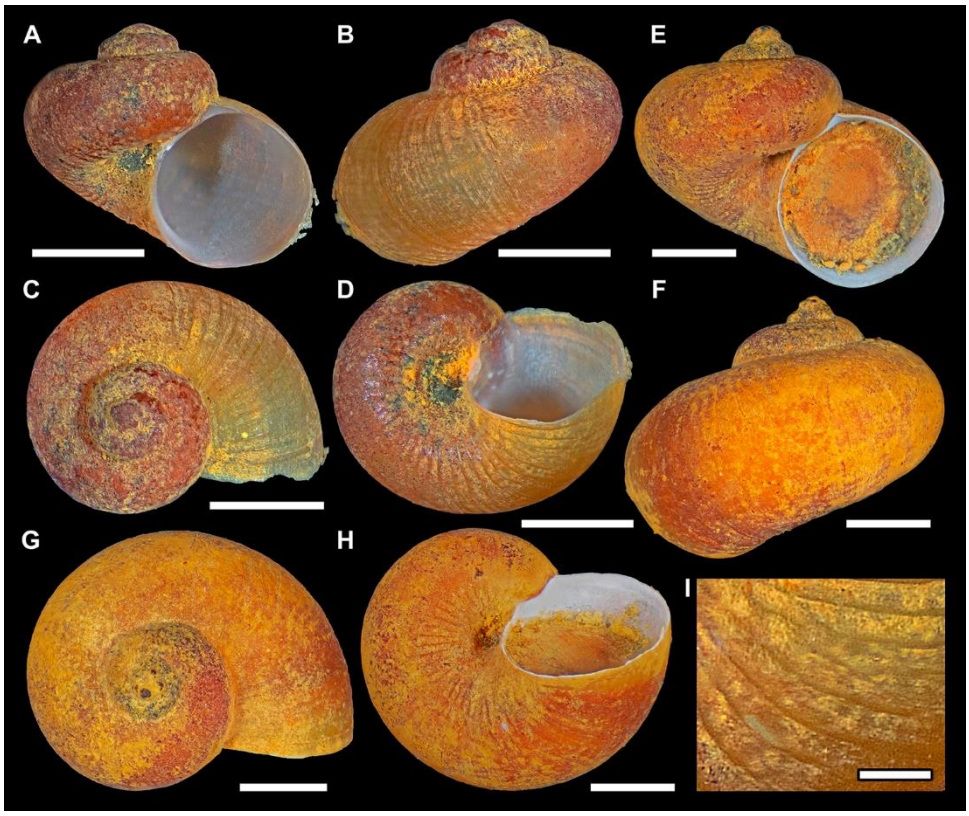

Figure 3

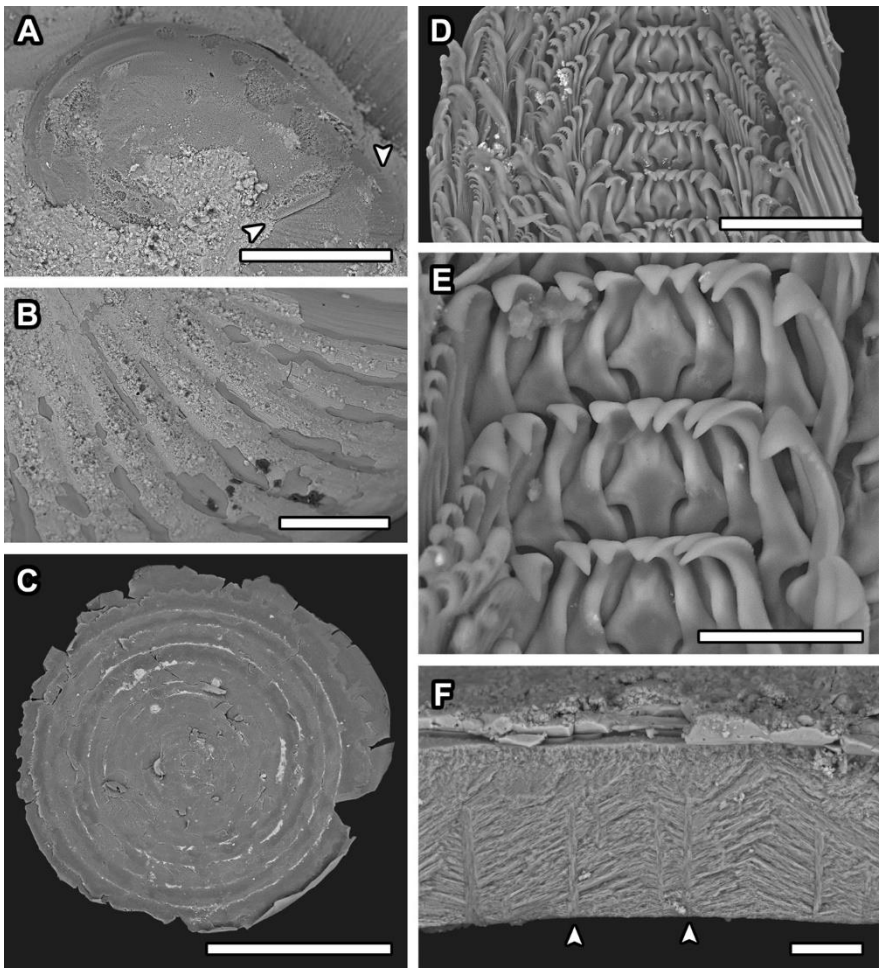

Figure 4

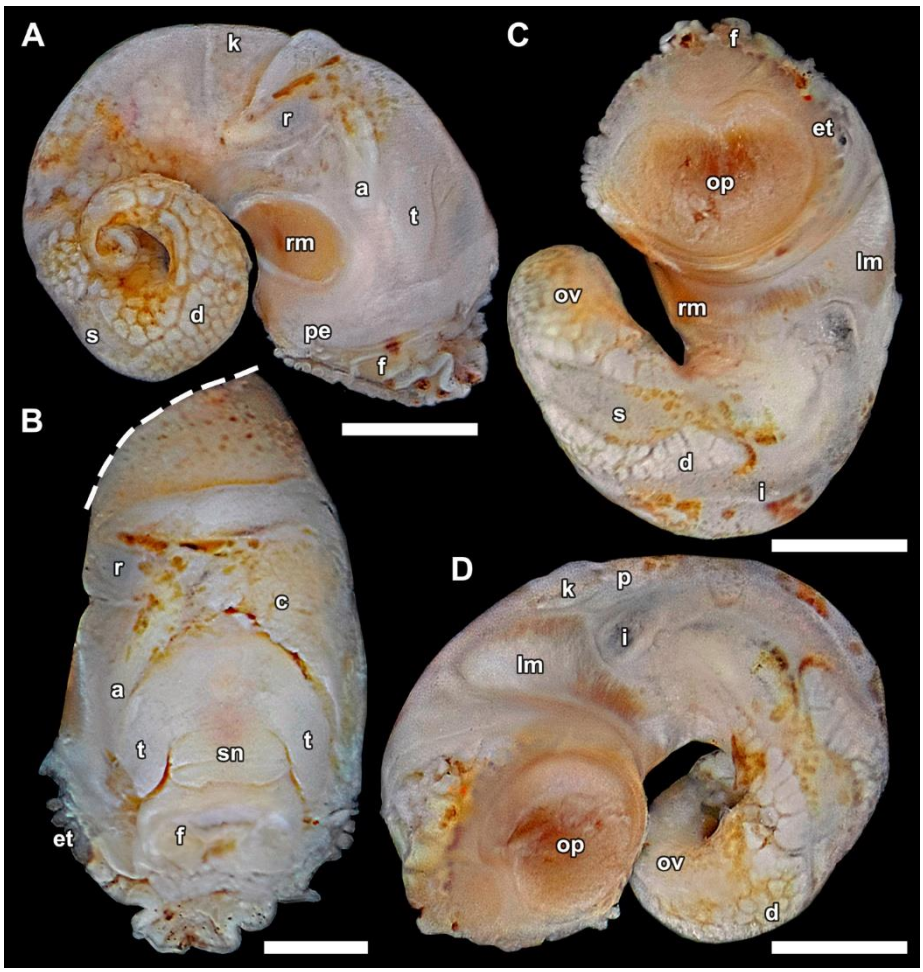

Figure 5

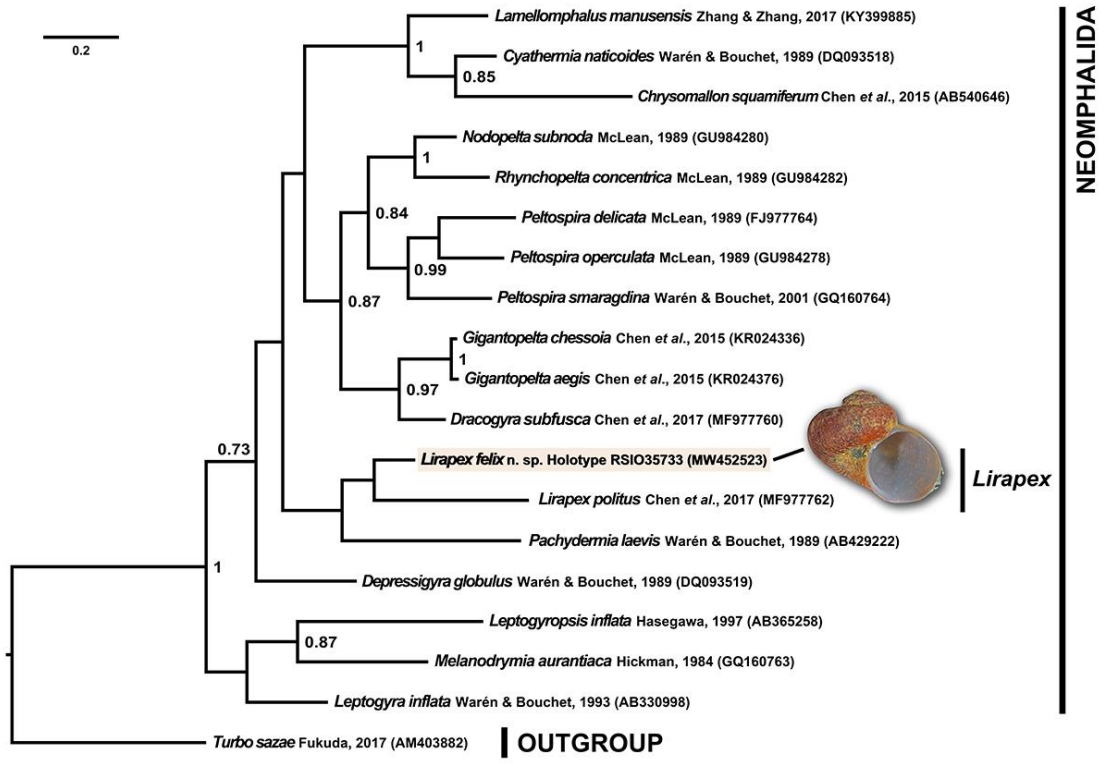
0.2
Lamellomphalus manusensis Zhang & Zhang, 2017 (KY399885)
Cyathermia naticoides Warén & Bouchet, 1989 (DQ093518)
Chrysomallon squamiferum Chen et al., 2015 (AB540646)
Nodopelta subnoda McLean, 1989 (GU984280)
Rhynchopelta concentrica McLean, 1989 (GU984282)
Peltospira delicata McLean, 1989 (FJ977764)
Peltospira operculata McLean, 1989 (GU984278)
Peltospira smaragdina Warén & Bouchet, 2001 (GQ160764)
Gigantopelta chessoia Chen et al., 2015 (KR024336)
Gigantopelta aegis Chen et al., 2015 (KR024376)
Dracogyra subfusca Chen et al., 2017 (MF977760)
Lirapex felix n. sp. Holotype RSIO35733 (MW452523)
Lirapex politus Chen et al., 2017 (MF977762)
Pachydermia laevis Warén & Bouchet, 1989 (AB429222)
Depressigyra globulus Warén & Bouchet, 1989 (DQ093519)
Leptogyropsis inflata Hasegawa, 1997 (AB365258)
Melanodrymia aurantiaca Hickman, 1984 (GQ160763)
Leptogyra inflata Warén & Bouchet, 1993 (AB330998)
Turbo sazae Fukuda, 2017 (AM403882)
OUTGROUP
Lirapex
NEOMPHALIDA
1
0.85
1
0.84
0.99
0.87
1
0.97
0.73
1
0.87